

# MINERAL PIGMENTS FOR PAPER: STRUCTURE, FUNCTION AND DEVELOPMENT POTENTIAL

Patrick A.C. Gane  
Omya AG  
CH 4665 Oftringen  
Switzerland

## INTRODUCTION

Pigments in paper play three major roles. The optical properties of pigments are used to enhance opacity and brightness of the paper. They are chosen to impart improved end-use characteristics, such as smoothness and printability: the latter being a function of the inter-particle pore structure and surface chemistry. They have maximum effect when incorporated in coatings with natural and synthetic binder systems. Thirdly, they have been, and continue to be, an economical way of extending the fibre with reduced fibre content by replacing fibre with filler.

Papers today contain high levels of mineral pigments ranging from 35 %w/w in woodcontaining supercalendered grades up to 50 %w/w in multi-coated woodfree grades. The level of pigmentation used simply as filler is limited by loss of mechanical properties, such as strength and stiffness, and the propensity for dusting and piling in the printing and converting of the final product. It is because of these drawbacks associated with uncoated papers relying on filling alone that coated grades have emerged and flourished.

To understand the function of fillers, coatings and their interactions with fibres and the papermaking chemical environment, we shall outline the fundamental structure of typical mineral pigments and develop the concepts which are applied today. Based on this foundation we shall seek some pointers to the future development opportunities that can be expected to form the next generation of information-carrying surfaces: and these should remain paper!

## PIGMENT STRUCTURES: morphology and crystallography

Naturally occurring mineral pigment deposits were formed either directly in situ by organic life forms or by geological and geophysical transformations of rock structures, or a combination of these.

### *Clay minerals*

The structure of clay minerals has been determined largely by X-ray diffraction methods. The essential features of *hydrous layer silicates* were revealed by various workers including Charles Mauguin, Linus C. Pauling, W.W. Jackson, J. West and John W. Gruner in the late 1920s to mid 1930s. These structures showed themselves to be continuous two-dimensional tetrahedral sheets composing  $\text{Si}_2\text{O}_5$ , with  $\text{SiO}_4$  tetrahedra linked by the sharing of three corners of each tetrahedron to form an hexagonal mesh pattern, Fig. 1.

Frequently, silicon atoms in the tetrahedra are partially substituted by aluminium. The oxygen at the apex (fourth corner) of the tetrahedra is usually directed normal to the sheet and forms part of an adjacent octahedral sheet in which the octahedra are linked by the sharing edges, Fig. 2. The junction plane between tetrahedral and octahedral sheets consists of the shared apex oxygen atoms of the tetrahedra and unshared hydroxyls that lie at the centre of each hexagonal ring of the tetrahedra and at the same level as the shared oxygen atoms, Fig. 3. Typical cations that coordinate the octahedral sheets are  $\text{Al}^{3+}$ ,  $\text{Mg}^{2+}$ ,  $\text{Fe}^{3+}$  and  $\text{Fe}^{2+}$ . If divalent cations ( $M^{2+}$ ) are in the octahedral sheets, the composition  $M^{2+}/3 (\text{OH})_2\text{O}_4$  is formed and all the octahedra are occupied. If there are trivalent cations ( $M^{3+}$ ), the composition is  $M^{3+}/2 (\text{OH})_2\text{O}_4$  and two-thirds of the octahedra are occupied, with the absence of the third octahedron. The former type of octahedral sheet is called trioctahedral, and the latter dioctahedral, Fig. 4.

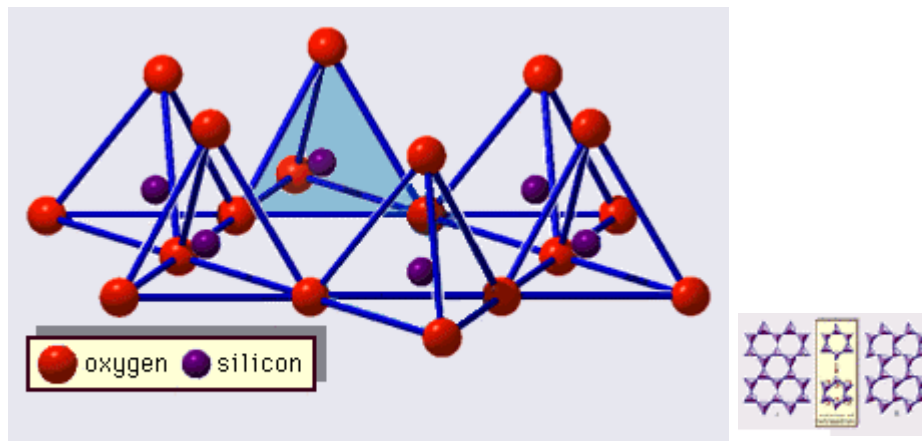


**Fig. 1** Single silica tetrahedron (shaded) and the forming of the hexagonal sheet structure<sup>1</sup>.

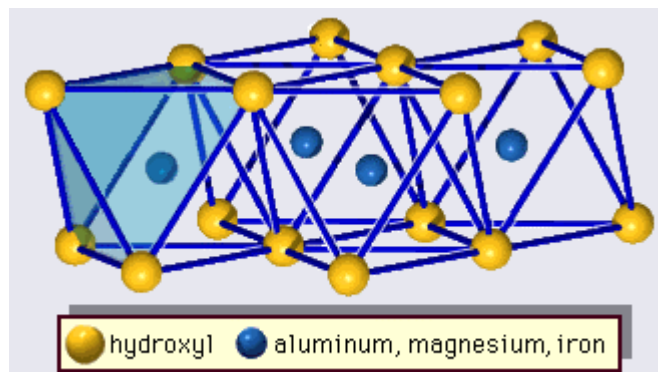


**Fig. 2** Single octahedron (shaded)<sup>1</sup>.

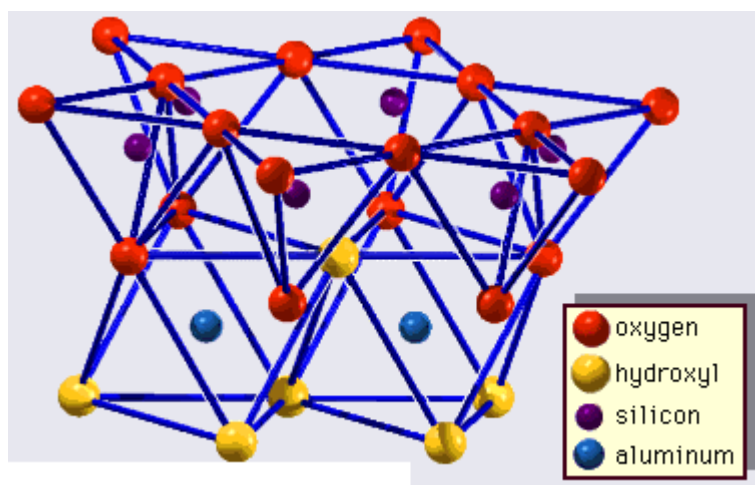


**Fig. 3** Structure of a 1:1 layer silicate (kaolinite)<sup>1</sup>.

<sup>1</sup> The schematics of the crystal structure for layered silicates are taken from Encyclopaedia Britannica.

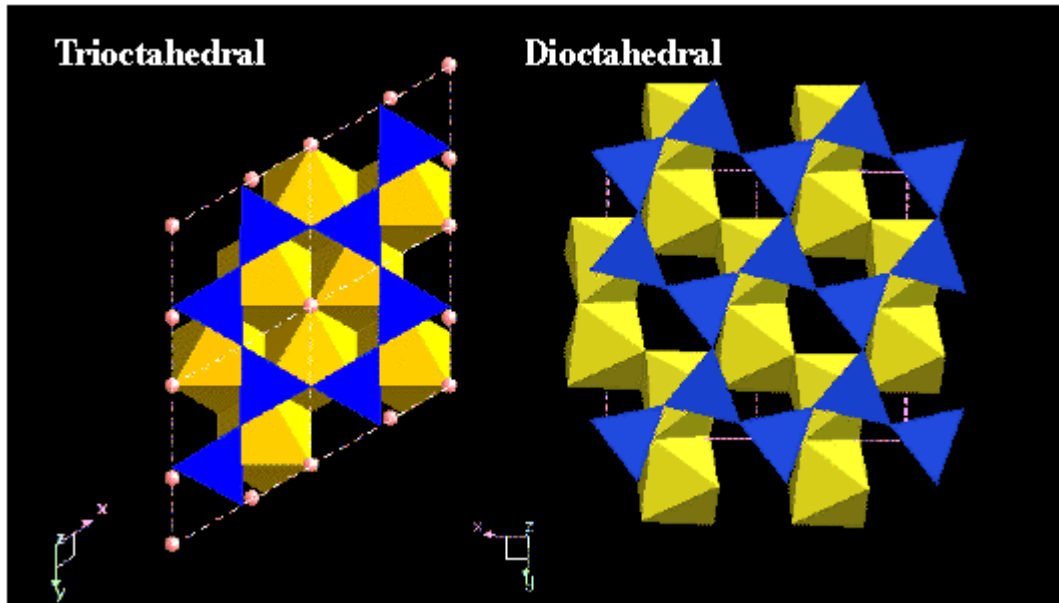


**Fig. 4** 3D schematic of trioctahedral and dioctahedral structures<sup>2</sup>.

There are two major types for the structural "backbones" of clay minerals called silicate layers. The unit silicate layer formed by aligning one octahedral sheet to one tetrahedral sheet is referred to as a 1:1 silicate layer, and the exposed surface of the octahedral sheet consists of hydroxyls. In the second type, the unit silicate layer consists of one octahedral sheet sandwiched by two tetrahedral sheets that are oriented in opposite directions and is termed a 2:1 silicate layer, Fig. 5.

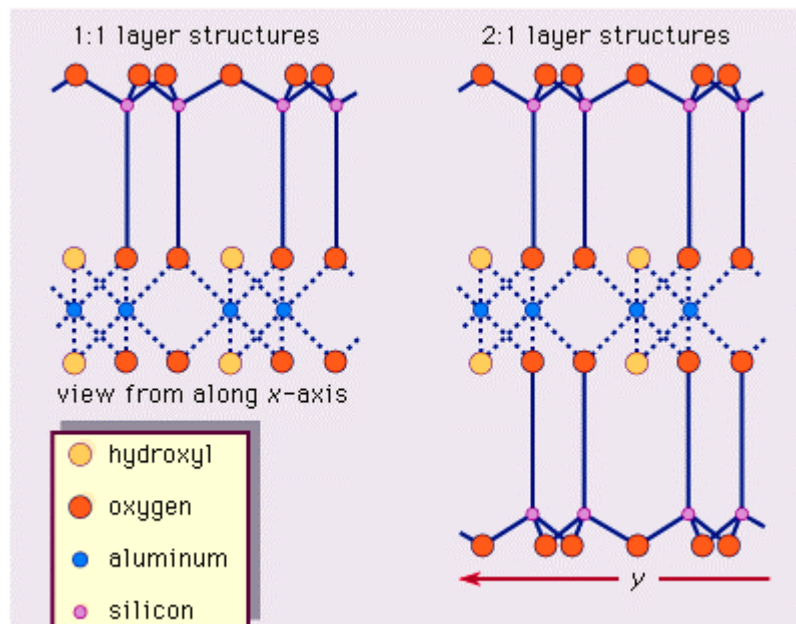


**Fig. 5** Schematic of a 1:1 and 2:1 layer silicate<sup>1</sup>.

Real structures of clay minerals contain substantial crystal strains and distortions, which produce irregularities such as deformed octahedra and tetrahedra rather than polyhedra with equilateral triangular faces, ditrigonal symmetry modified from the ideal hexagonal surface symmetry, and puckered faces instead of the flat planes made up of the basal oxygen atoms of the tetrahedral sheet. One of the major causes of such distortions is dimensional "misfits" between the tetrahedral and octahedral sheets.

*Kaolin* (kaolinite), so-called after the first known use for pottery manufacture by the Chinese of white aluminosilicates found in the Kao-Ling district, is a 1:1 layer silicate and has for many years been the major pigment form used in acid papermaking to add smoothness and opacity to paper. It has an idealised structural formula of  $\text{Al}_2\text{Si}_2\text{O}_5(\text{OH})_4$ , Fig. 6. Because of its hexagonal plate-like structure it carries naturally differing surface chemistry/charge on the edges compared with the faces. At low pH, the surface charge at the edges is cationic while that on the faces is anionic. This changes at higher pH as the edge cationicity becomes neutralised. Processing of kaolin takes advantage of these charge density configurations allowing the refinement through an edge-to-face flocculation-deflocculation sequence as a function of pH. Shape and surface chemistry also aids retention within the forming fibre matrix during papermaking and retention polymer adsorption further develops this particle entrapment.

The morphology of kaolin can differ greatly from source to source. Its formation from the degradation of granite can be seen directly when found in primary deposits within the granite matrix, such as occur in Cornwall in Southwest England. Here the mineral is won by washing the kaolin from the partially degraded friable granite. Primary deposit kaolin can be relatively pure with other mineral contaminants confined generally to smectites at the fine particle size, mica at the coarser end and some discoloration due to iron occupancy in the crystal structure. The crystal form is well-defined with high aspect ratio platelets occurring throughout the size distribution of particles especially at the fine end of the size distribution. On the other hand, secondary deposit kaolins, such as are found on what were the prehistoric coastal planes of Georgia in the United States of America, have undergone transportation from the primary formation site, usually by water transport, and become worn due to abrasive attrition. Sedimentary beds form together with organic, humic deposits leading to reduced aspect ratio of the finest particles and a tendency for yellowing and slime formation within the colloidal fraction. Secondary deposit kaolin tends therefore also to be finer.

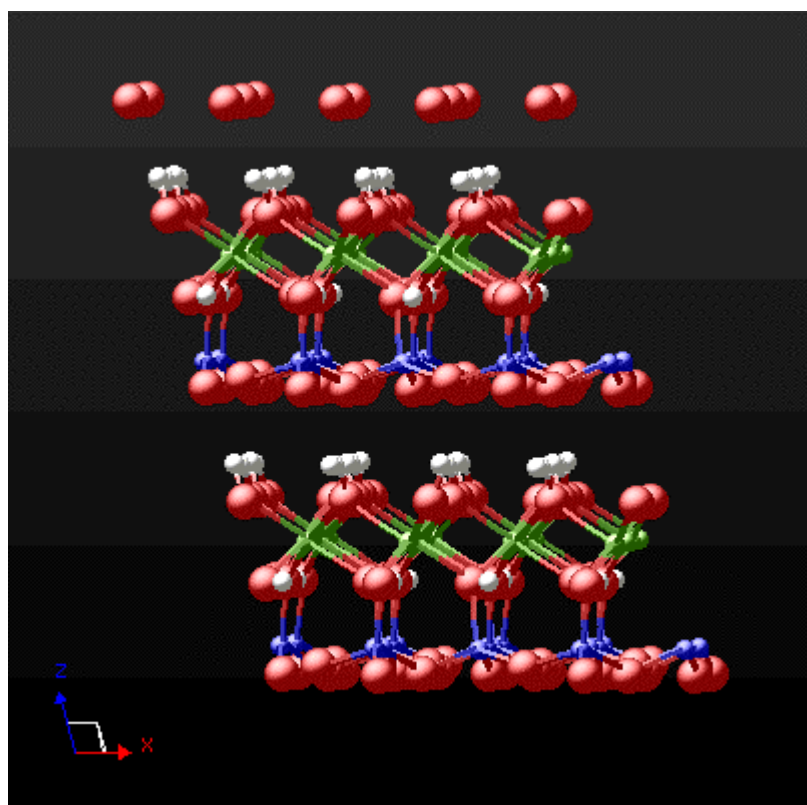


**Fig. 6** The 1:1 silicate layer structure of kaolinite<sup>2</sup>.

Specialised forms of kaolin have been developed to enhance optical properties and to form bulky structures. So-called structured kaolins range from simple charge stabilised flocs through to calcined clays in which the dehydration of the hydroxy substitution leads to a crystal morphology strain releasing electrons by oxidation and providing a brighter product.

<sup>2</sup> As published by the Mineralogical Society

*Talc* is another frequently used platy pigment structure and is an example of a 2:1 layer silicate with an idealised structural formula expressed as  $Mg_3Si_4O_{10}(OH)_2$ , Fig. 7. The layers of talc are electrostatically neutral and are held together via van der Waals bonding. As a result of neutrality, talc is strongly oleophilic and therefore its hydrophobicity creates challenges in dispersability in aqueous systems. However, the surface properties are very valuable in respect of adsorption of stickies and other aliphatic compounds for pitch control in papermaking and, as we shall see later, the attractiveness toward oils, toluol and esters make it a useful additive in coatings for control of offset and rotogravure printability.

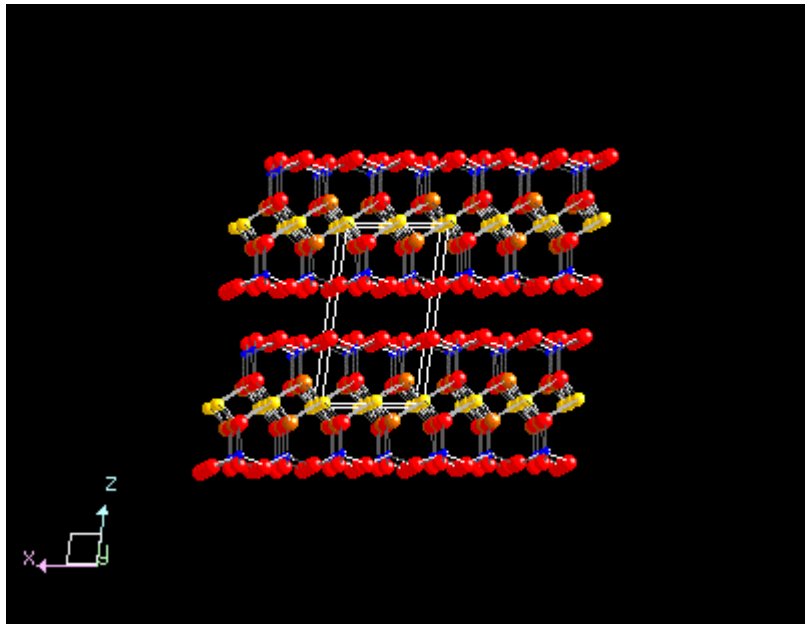


**Fig. 7** The 2:1 layer silicate structure of Talc<sup>2</sup>

*Calcium Carbonate* can be found in nature in a vast myriad of types and forms. It is a structural component of most skeletal creatures which have lived on earth and is part of an unbroken cycle and so, in principle, is inexhaustible. The majority of deposits were formed by the capture of  $CO_2$  from the atmosphere by microorganisms which combined the dissolved gas with calcium ions to form their exo-skeleton providing protection and structural support. Consumption by higher vertebrates also captured the mineral in their bone skeletal structures. Deposits of coccoliths formed chalk beds at the sea bottom which later became transformed under pressure to form limestone and in some cases combining high pressure and temperature to promote recrystallisation into marble, the hardest and brightest form of calcite.

Calcite is  $CaCO_3$ . The Ca atoms (red), Fig. 8, are at the corners and body centre position of a trigonal lattice with  $\alpha = 46$  degrees and a lattice parameter of 0.6361 nm. The planar  $CO_3$  (blue) radicals are at about 1/4 and 3/4 the distance along the major diagonal. Each Ca atom has 6 closest oxygen atoms. The  $CO_3$  groups are arranged in a flat triangle with the C in the middle.

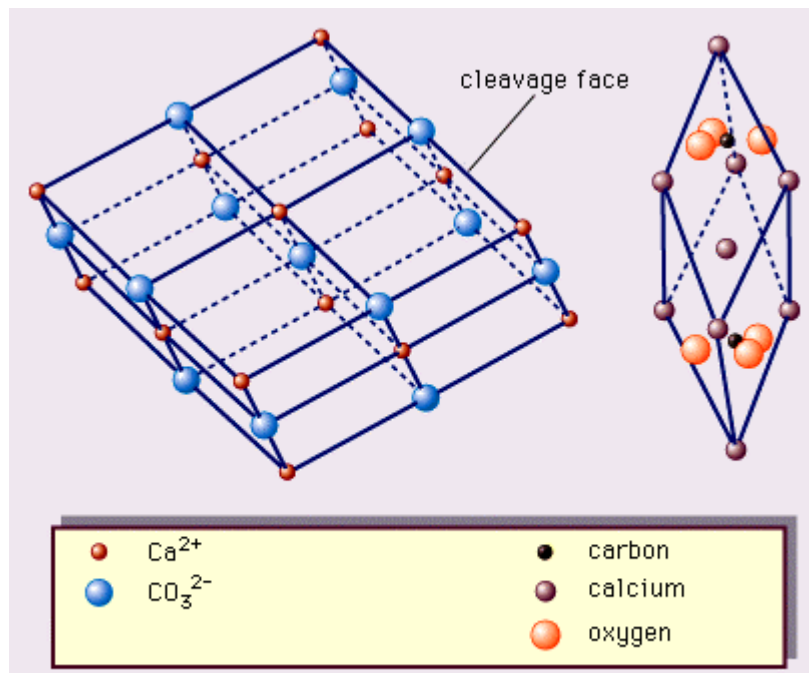
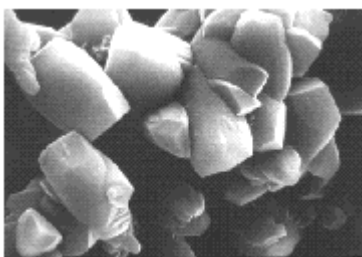


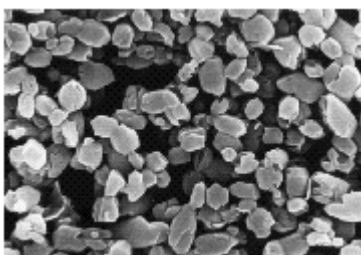
**Fig. 8** The crystal structure of calcite<sup>3</sup>. This schematic diagram shows both (left) the true unit cell (the acute rhombohedron, which contains 2[CaCO<sub>3</sub>]) and (right) an alternative cell based on the cleavage rhombohedron.

Synthetic calcium carbonate is made by firstly reversing the natural process endothermically, driving off the CO<sub>2</sub> once more, then subsequently slaking in water exothermically followed by reprecipitation of the carbonate by bubbling through CO<sub>2</sub>. This can be made under carefully controlled concentration and temperature conditions to form any of the commonly useful crystal habits of calcium carbonate: rhombohedral calcite (as above and as found in marble), prismatic, spherically agglomerated and scalenohedral ("cigar"-shaped crystals occurring frequently in a clustered form), Fig. 9. The aragonitic (needle form) habit is more difficult to produce and is generally reserved for coating applications.

In practice, the batchwise precipitation process demands sophisticated control systems to maintain satisfactory consistency, and in coating applications this is an aspect which continues to limit its use severely as ground carbonates progress to supplant kaolin completely in some woodfree grades.

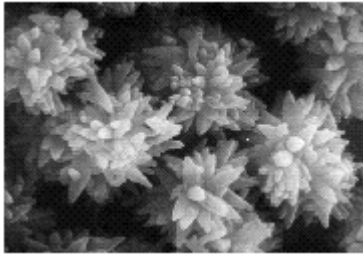


Rhombohedral calcite

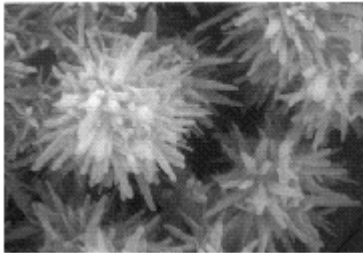


Prismatic

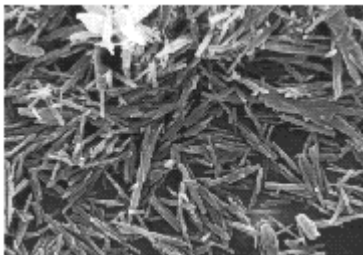
<sup>3</sup> Encyclopaedia Britannica.



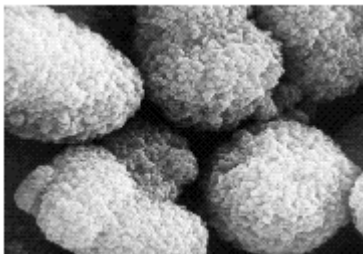
Scalenohedral



Clustered aragonite



Aragonite



Spherically agglomerated

**Fig. 9** Commonly found forms of synthetically precipitated calcium carbonate<sup>4</sup>.

*Functional pigments* play an important role in papermaking both for their properties as required by the end-use and for their process-enhancing qualities. Many are of high surface area acting as either speciality chemical adsorbers, e.g. bentonite (montmorillonitic smectite) - a highly platy laminate structure of the 2:1 layer silicate type with a slight anionic charge density due to ionic substitution, or precipitated silica which combines high surface area with large interparticle pore volume. These latter types are often referred to as colloidal particles due to their microscopic nature and due to their tendency to interact with other microscopic species creating colloidally stabilised dispersions and gels.

#### **PARTICLE SIZE: its importance, definition and production control**

The particle size and distribution of sizes of a mineral pigment are determined traditionally using the sedimentation resistance of a particle of mass,  $m$ , flowing through a fluid of viscosity,  $h$ , reaching an equilibrium velocity,  $v$ , under the action of a gravitational acceleration,  $g$ , i.e. the Stokes' diameter or equivalent spherical diameter ( $d = 2a$ ).

---

<sup>4</sup> Electronmicrographs <http://www.mineralstech.com/pccmorphologies.html>

$$mg = -\mathbf{F} = -6\pi\eta r v \quad [1]$$

This is a practical but crude description when it comes to particles of complex shape and it assumes complete dispersion of the particles. Observation of the Stokesian dynamic can be made using either a simple extraction and density determination as a function of height, suitable for coarse pigments, or by measuring the absorption of X-radiation using the Beer-Lambert transmission intensity decay,  $I/I_0$ , as a function of path length through the particle,  $l$ , for an absorption constant of  $1/t$ ,

$$I = I_0 e^{-l/t} \quad [2]$$

Alternatively, in some cases, dynamic light scattering techniques can be used, in which the exponential decay of the autocorrelated intensity fluctuation function can be used to obtain a diffusion coefficient,  $D$ , which again can be related to the Stokesian drag to obtain a particle size using,

$$d = \frac{kT}{3\pi\eta D} \quad [3]$$

where  $k$  is the Boltzmann constant and  $T$  the absolute temperature. Dynamic light scattering, however, is limited to those particles truly undergoing Brownian motion which confines the technique to particles  $< 2 \mu\text{m}$  at room temperature but may be raised to  $< 5 \mu\text{m}$  if dilute suspensions (vanishing solids content) at elevated temperatures are used.

As we shall see later, optically and chemically active particulates have optimal particle size criteria based on the interaction with light and the activation energy distribution densities, respectively. Pore structures and geometries define the absorption properties of paper. To achieve optimal properties it is necessary to control particle size and shape accurately and reproducibly. For synthetic pigments this is part of the precipitation or forming kinetics but for naturally occurring minerals various comminution techniques are used. The action of grinding can take several forms ranging from delamination of layered minerals, through frictional attrition to breakage.

#### (i) Delamination of platy structures

If we consider the separation of platelets of, say, kaolin or talc, then we need to understand the effect on the number of particles present after the process and the observed change in measured parameters such as particle surface area and mass distribution of the particles before and after processing.

In Fig. 10 we can follow the action of splitting a particle made of two laminates into their separate laminar parts. Conservation of mass means that we halve the mass of each particle and therefore double the number of particles with a doubling of the specific surface area, i.e. the surface area per unit weight of the pigment. Provided there is not attrition or breakage, theoretically the measured particle diameter will remain constant while the thickness will decrease as surface area increases. The effect on equivalent spherical diameter is related to the aspect ratio of the particles,  $d/t$ , where  $d$  is the major dimension (diameter of the platelet) and  $t$  its thickness, which, for high aspect ratio, can be expressed as:

$$\text{equivalent spherical diameter} = d \tan^{-1}(d/t) \quad [4]$$



## High aspect ratio kaolin

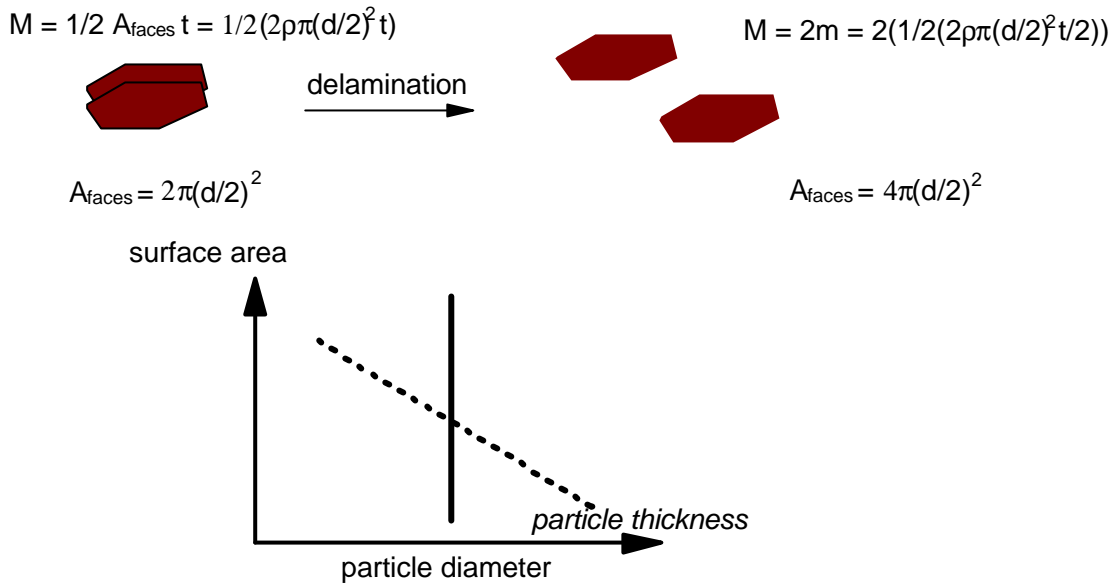


**Fig. 10** Delamination of platy pigments.

### (ii) Grinding of needle-like particles

Similarly, we can follow the properties of needles as they are broken during grinding as shown in Fig. 11.

## Needle-shaped particles

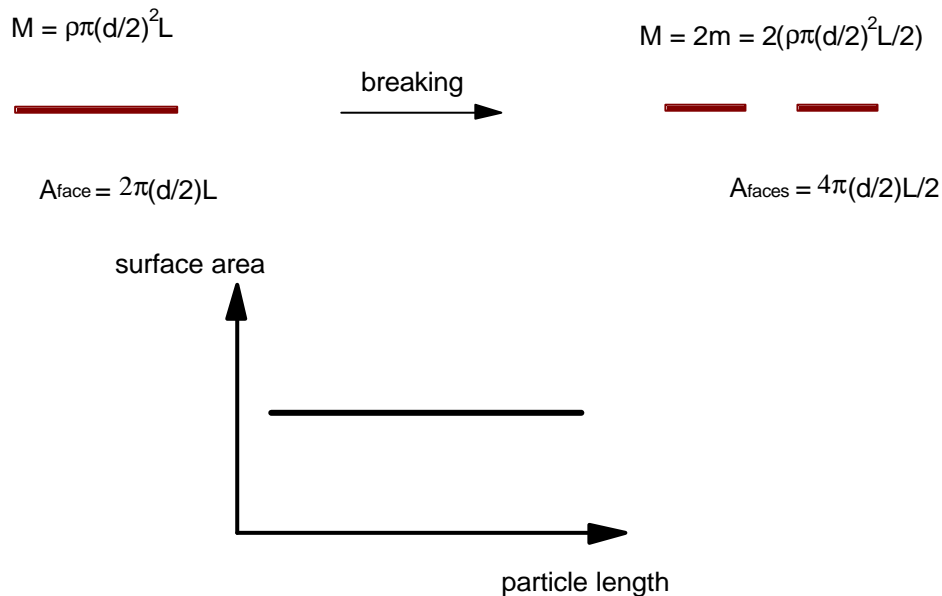


**Fig. 11** Breakage of needles during grinding.

Now we see that specific surface remains virtually constant while the particle length distribution shortens. In this case, the standard particle size measurement will record an equivalent spherical diameter as follows:

$$\text{equivalent spherical diameter} = C.L \quad [5]$$

where  $C$  is a constant and  $L$  is the needle length for constant thickness,  $d$ .

**(iii) Grinding of "spherical" morphologies**

This case is the most similar to the standard grinding of natural calcium carbonate. The rhombohedral calcite crystals approximate well to spheres.

In this case, we see from Fig. 12 that a breakage of a spherical particle into two forms a more complex power law relationship with respect to particle size. The new surface area increases by a factor of  $2^{1/3}$  where the new distribution of diameters,  $d'$ , follows a cubed relation,

$$d'^3 = \frac{1}{2} d^3 \tag{6}$$

and the equivalent spherical diameter is closely related directly to the actual diameter,  $d$ . Surface area, therefore, increases exponentially with grinding and this factor defines that fine ground spherical particles have the strongest interaction potential, for example, in respect to absorption and sensitivity to printability.

**Spherical particles**

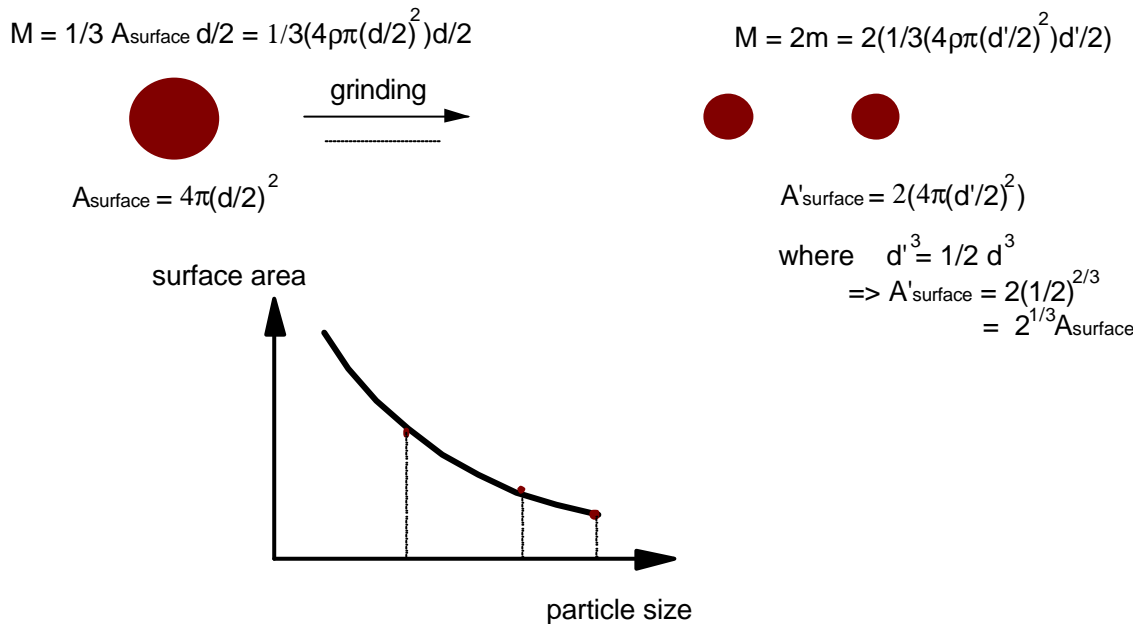


**Fig. 12** Comminution of spherical particles.

**Economic production factors for calcium carbonate**

An economic contrast must be understood between the energy input required for comminution and the endothermic reversal of the natural crystallisation employed in the manufacture of synthetic precipitated calcium carbonate. This is an environmental and straightforward business question and depends strongly on the logistic and siting of raw materials in relation to the consumer, and which energy form can be utilised. For example, hydro-electric power in regions of non-vegetative growth is relatively cheap and more environmentally acceptable, say, as found in mountainous regions, where often natural mineral deposits are to be found. This is to be contrasted with the extensive logistic required for transportation across vast planar land regions of low value grades. In these circumstances on-site facilities hold an attraction. Each case must be studied and the best solution sought from not only a performance stand-point today but increasingly from the environmentally acceptable approach. Research in calcium carbonate will mean that  $\text{CaCO}_3$  from either natural or from synthetic sources will be technically advancing and the options will therefore foreseeably remain completely flexible.

## PIGMENTS IN AQUEOUS SYSTEMS

Surface active particles develop an adsorption potential for water, ions and molecules of a variety of molecular weights, surface energy and charge. The natural dispersability of kaolin at neutral to alkaline pH, for example, has been historically used to provide like-charge repellancy, and hence particle-particle separation, ideal for maximising the effect of interparticle voidage and adsorption potential. When used as filler together with fibres, this "natural dispersability" of kaolin is then reversed in the acid papermaking environment encouraging retention through flocculation.

For high solids content, this effect can be enhanced further for kaolin by adsorbing selectively on the particle edges anionic dispersant polymers, usually in the form of the soluble salts of polyacrylic acid, Fig. 13. This increased anionicity stabilises the dispersion over the complete range of pH relevant to papermaking.

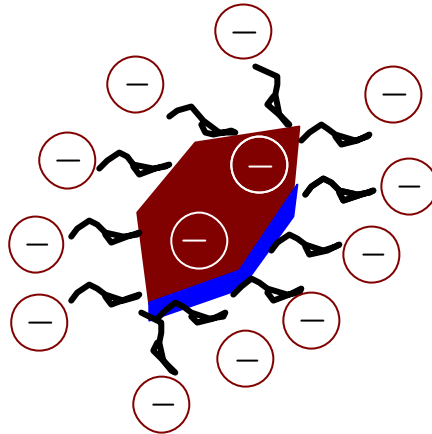


**Fig. 13** Anionically dispersed kaolin.

In the case of calcium carbonate, Fig. 14, dispersant polymers can be adsorbed onto the naturally slightly cationic surface through a complex interaction with adsorbed water and the precipitation of insoluble salts of anionic polymers, such as polyacrylic acid.

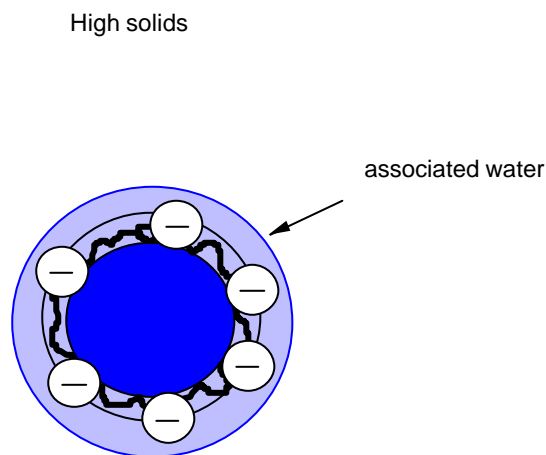


**Fig. 14** Adsorbed dispersant and associated water layer on a calcium carbonate particle.

Electrostatic stabilisation is long-range in its action potential and determines the initial barrier against collapse into a Lennard-Jones type potential, which describes the balance between van der Waals and London attraction forces and the steric barrier provided by adsorbed species.

## DLVO potential

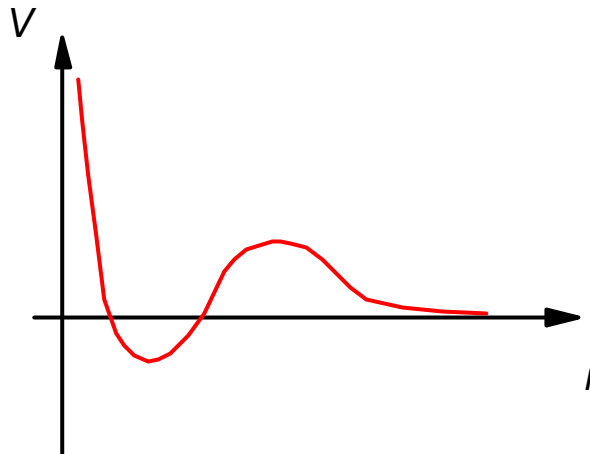


**Fig. 15** Representation of the stabilisation potential of a dispersed pigment.

The potential is usually described by the DLVO (Derjaguin, Landau, Verwey and Overbeek) theory, which operates quite well as a working model. However, in most papermaking operations, high levels of soluble ions and, more particularly, soluble charged polymers are present (e.g., CMC, hemicellulose etc.) which act to form concentrated regions of charge- and polymer-rich hydrophilic species. These in turn create osmotic pressure differentials which lead to a depletion of the electrostatic water layer around the particles. This would have to be balanced by strongly hydrophilic adsorbed polymers which retain the associated water layer around the particle if electrostatic stability were to be maintained. Therefore, in practice, the long-range electrostatic force, with its predicted flocculation minimum does not occur as readily as expected from the pure DLVO theory - [clearly, the system of dissolved species and the osmotic effect could be removed thus re-establishing the validity of DLVO, but many of the specialised additives are present for other functional reasons]. Concentrated dispersions (slurries) of pigments are therefore stabilised by the combination of steric, electrostatic and osmotic forces. Papermaking processes often require the subsequent destabilisation of these forces to create retention and flocculation for example, and so it is valuable to have a good working knowledge of the predominant force in each application in order to have full control over the process. The simplistic practice of balancing the surface electrical  $z$  potential is often insufficient to determine the interactions in papermaking as it assumes purely electrostatic stabilisation.

Dispersion of hydrophobic minerals, such as talc, is achieved by the use of surface active agents (surfactants) and polymers. The surfactant acts to promote wetting of the surface and compatibility with other mineral and binder dispersions is obtained by secondary adsorption of anionic dispersant. Specialised combined polymers are tending to take over from this complex system. However, the unique property of the pigment, i.e. its hydrophobicity, is to a large extent lost. Developments using costructuring in which other anionically dispersed hydrophilic pigments are used to disperse the hydrophobic talc are discussed later, in which the unique surface properties of the talc can be retained and used to advantage.

## OPTICAL PROPERTIES

Light is described variously in both quantum and continuous forms. The apparent wave nature of light transmission is used to signify the phase correlation properties between successive photons, i.e. the ability to interfere, creating reinforcement or cancellation of the propagating light energy.

When light encounters an object, the interaction is strongly dependent on the relation between the wavelength of the light and the size and atomic structure of the respective object. Macroscopically this interaction is defined by the refractive index,  $n$ , of the material, i.e. its bending and reflective power, Fig. 16.

$$n \sin r = \sin i$$

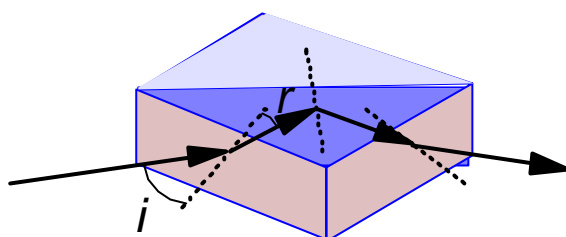


**Fig. 16** Refractive index,  $n$ , effects the bending and reflective power of an object changing the angle of incidence,  $i$ , into the angle of refraction,  $r$ .

To maximise the apparent whiteness and opacity of the paper, the pigment must on the one hand reflect strongly (Fresnel specular reflection) to achieve uniformity of gloss, and on the other hand should scatter light - the snow-white effect. Light scattering is really a quantum phenomenon but is variously described using continuum models such as Rayleigh scattering (diffraction limited) and Mie scattering (cross-section of interaction). The maximum scattering cross-section is a function of refractive index and the wavelength (energy) of light. For common pigments of refractive index,  $n = \sim 2.5 - 2.7$ , the light scattering goes through a maximum as a function of particle size and the void size between the particles, Fig. 17.

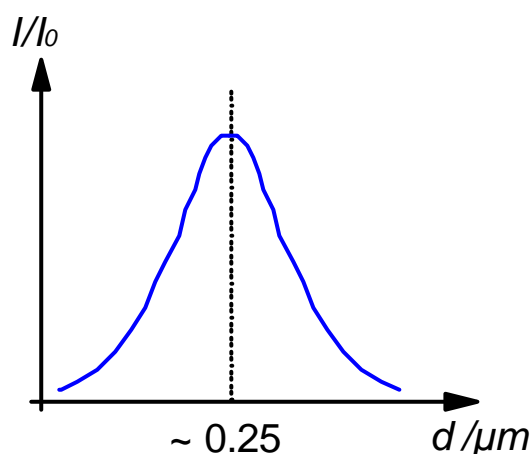


**Fig. 17** Dependency of light scattering as a function of particle size in a packed pigment layer.

This maximum in light scattering is strongly dependent on interparticle boundary properties and especially upon the refractive index contrast gradient at the particle-particle and particle-air boundaries. The greater the contrast over a distance close to the wavelength of the light, the greater is the scattering power.

It is easier to maximise scattering in coatings than when using a pigment as a filler distributed amongst a fibre network due to the important role played by the interparticle packing characteristics occurring at the maximum volume packing fraction in an immobilised coating layer compared with the low contrast occurring discretely at the particle-fibre contacts.

Structures are made from clustered or aggregated pigments to enhance the interparticle effect and to provide higher opacity when used in filler applications. An early example of a structured pigment is calcined clay, in which the feed particle size is chosen to be close to the packed particle scattering optimum of  $\sim 0.25 \mu\text{m}$ , i.e. as shown in Fig. 17, and then fused together under elevated temperature to form an aggregate particle with internal voidage designed to develop the light scatter. As we saw in Fig. 9, other pigments such as calcium carbonate can be structured or nested to form high scattering composites. Particles of different brightness and light scattering

properties can be combined in costructures to enhance the brightness of darker minerals or to increase the scattering power of lower refractive index materials, Fig. 18.

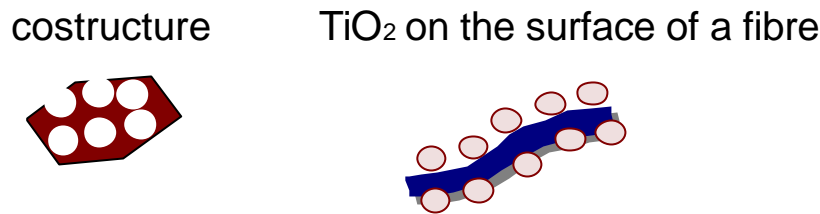


**Fig. 18** The principle of costructuring and the distribution of high refractive index particles on low contrast substrates.

To model the light interactional properties of pigments using the combined theories of Rayleigh and Mie is intractable for the complexity of geometries and component mixes we find in paper composites. The model of Kubelka and Munk provides a working tool with which to describe the important effects of pigments and paper systems. The model breaks the problem down into two simple components which describe the light backscattering coefficient,  $S$ , and the light absorption coefficient,  $K$ . By applying combined measurements of brightness over an infinite layer of the test material compared with a defined layer contrasted over a black background (or of defined brightness) the parameters can be measured experimentally. High pigment brightness relies on high  $S$  and low  $K$ . Opacity, however, can be achieved by a combination of optimal  $S$  and  $K$ . The challenge today is that the market demands high brightness and so opacity must come from pigments with the highest possible light scattering coefficient often in combination with pigments of very high refractive index, e.g. mixes of bright calcium carbonate and high refractive index  $\text{TiO}_2$ . To maximise the efficiency of the highly absorbing  $\text{TiO}_2$ , it is necessary to ensure the thin layer distribution of the particles over substrates using the minimal thickness of the layer, i.e. no more than a single particle thickness, to avoid the absorption of light before being scattered from lower layers of  $\text{TiO}_2$ . Such absorption is wasteful of scattering power.

## POROSITY AND STRUCTURE-FLUID RELATIONSHIPS

A main target end-use for paper and coated board is to carry and transmit information. This information is imparted to the paper or board surface through the medium of printing. Most printing processes (apart from laser toner and wax transfer) involve the absorption of fluids in combination with the deposition (hold-out) of ink colouring pigments and/or the adsorption of coloured dyes.

Pore size distribution, connectivity and geometry play the major roles in determining the absorption characteristic of a wetting fluid entering pigmented porous structures. The surface energy of a material defines its "attractiveness" to the fluid, i.e. it relates to the surface tension of the fluid in relation to the wettability of that surface for the absorbing fluid. Once again we are dealing with molecular interactions manifest on a macroscopic scale. A full analysis requires a complete transition from continuum roughness criteria to quantum mechanical interactions. Macroscopically, the phenomenon is described in terms of the contact angle,  $q$ , and the liquid-vapour interfacial tension,  $g_{LV}$ , such that a Laplace pressure difference is developed through the curvature of a liquid front induced by the wetting of the pore walls by the fluid. We can consider this geometry as forming an "effective" capillary of radius  $r$ ,

$$\Delta P = \frac{2g_{LV} \cos q}{r} \quad [7]$$

Traditionally, a capillary equilibrium is understood to develop between the absorbing Laplace pressure [7] and the resistive pressure drop,  $\Delta P$ , caused by the fluid viscosity at a flow rate of,  $V/t$  (where  $V = \pi r^2 x$ ), occurring at a point,  $x$ , along the capillary, described in terms of the Hagen-Poiseuille equation,

$$\frac{V}{t} = \frac{pr^4 \Delta P}{8\eta x} \quad [8]$$

such that, equating the magnitudes of the pressure differentials at equilibrium in equations [7] and [8], we obtain the well-known Lucas-Washburn expression,

$$x^2 = \frac{r g_{LV} t \cos \theta}{2h} \quad [9]$$

giving the expected  $\sqrt{t}$  relationship for the amount of fluid absorbed as a function of time.

However, there is a problem when attempting to transfer this equation into the field of papermaking. Fluid is being absorbed over very short timescales into microstructures such as interparticle void structures. These short timescales are shorter than the time required to establish equilibrium viscous flow. Acceleration over the short times dominate the phenomenon, and the inertia of the fluid volume of density,  $\rho$ , must be considered. It is necessary to average over the  $t = 0$  discontinuity whilst this absorptive motion is established and having done this a description can be achieved using a variety of proposed equations based either on energy or momentum considerations. One such momentum model is that of Bosanquet (1923) and is given by,

$$\frac{d}{dt} \left( \rho r^2 \frac{dx}{dt} \right) + 8 \rho r x \frac{dx}{dt} = 2 \rho r^2 g_{LV} \cos \theta \quad [10]$$

This may be expanded using a Taylor series for the short time period showing a linear  $t$  relationship for the filling of individual pores up to a size of  $\sim 0.1 \mu\text{m}$  by typical printing fluids, such as water, toluene and light mineral oils within a timescale of  $\sim 10 \text{ ns}$ , which, via multiple connectivity with larger reservoir-forming pores, leads to a preferred pathway wetting phenomenon in which the large pore entries suffer an inertial retardation favouring absorption by the smaller pores.

$$x = t \sqrt{\frac{2 g_{LV} \cos \theta}{r \rho}} \quad [11]$$

An illustrative example of the preferred pathway is shown in Fig. 19, in which a specially developed modelling software Pore-Cor<sup>5</sup> has been used together with the Bosanquet wetting algorithm to show the passage of fluid through the absorbing structure. The combination with suspected pore wall wetting of the larger connecting pores, gives a factor promoting a differential dynamic for those fine pore structures up to and including those pores just finer than the light scattering optimum. This compromise between absorption and light scattering power is the greatest challenge to pigment designers today and can only be reconciled through judicious use of particle packing, shape and surface energy characteristics.

One way forward is to consider the costructure approach shown in Fig. 18 between calcium carbonate and talcum in which the light scattering optimum is provided by the calcium carbonate particle size and interparticle void size whilst the oleophilic surface of the talc enhances the absorption process for printing ink oils. Such a costructure has finally broken the incompatibility between rotogravure printing and high scattering, high bright paper surfaces. Further development in surface chemistry of pigments will be the key to balancing the interesting properties of absorption and light scattering.

---

<sup>5</sup> Pore-Cor is a software program devised by the Fluid Interactions Group of the University of Plymouth, PL4 8AA, U.K.

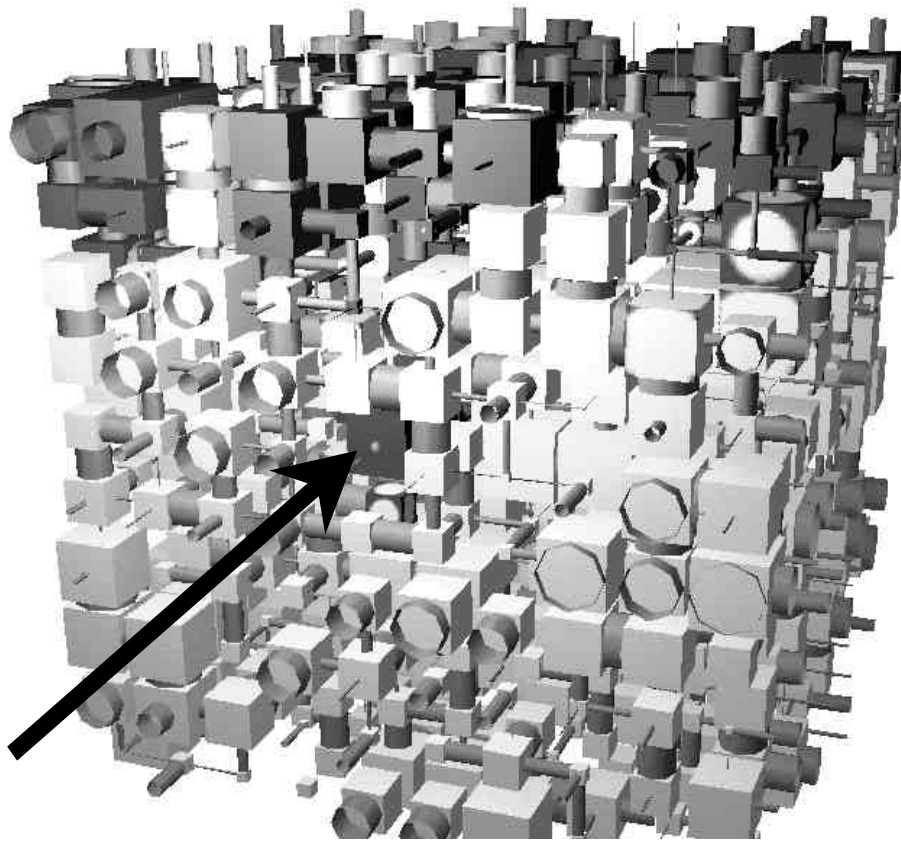


**Fig. 19** Schematic of a Pore-Cor cell filling under inertially controlled exclusion for water and a high porosity structure (porosity,  $\Phi = 28.02\%$ , pore row spacing,  $Q = 1.26\ \mu\text{m}$ )

### **Ink-on-paper tack force development as the indicator for ink fluid-paper structure interaction**

The Ink-Surface-Interaction-Tester (ISIT<sup>6</sup>) is an instrument regularly used to detect the tack force development of offset inks and varnishes on coated papers. This method provides an analysis of the tack behaviour from the initial tack rise caused by the ink fluid phase absorption into the structure until the final consolidation of the ink layer. Its action consists of measuring the time-dependent static force of retraction,  $F(t)$ , of an offset blanket-like material mounted on a roller which is brought under pressure into contact with a freshly printed paper sample.

The interpretation of the tack curve is shown schematically in Fig. 20. As we have seen above, the tack rise is controlled by the absorption of mineral oil into the finer pore structure in the coating (and the interpolymer absorption of oil in the latex binder used). The tack maximum is related to the microsmoothness of the coating surface and to the adhesion of the ink to the coating. The tack decay rate determines the consolidation/setting of the ink and depends on the oil drainage into the total pore volume actually available to the permeating oils, and, the level of tack decay can be influenced by the diffusive interaction between oil and latex whilst oxidative polymerisation of the resins can proceed. The available pore volume is a complex function of the preferred pathway wetting of the oil and the resistive structure build-up of the ink in contact with the coating surface.

<sup>6</sup> ISIT is a product name of SeGan Ltd., Perrose, Lantyan, Lostwithiel, Cornwall PL22 0JJ, U.K.



## Characterising the pore structure as the ink "sees" it

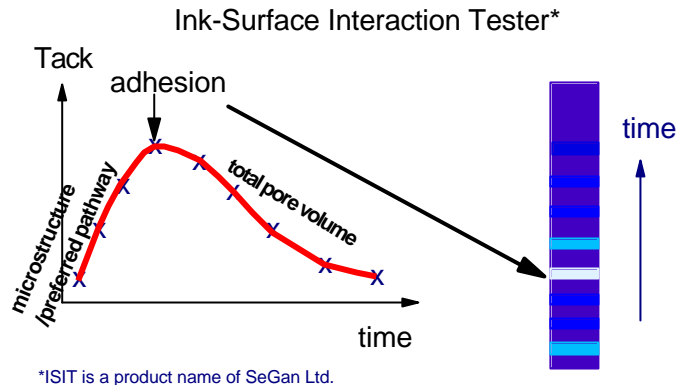


**Fig. 20** Schematic interpretation of the tack curve.

### Tack rise records the viscosity and solids concentration increase of the ink

Using an extensional model, the viscosity of the ink is derived from a process integral of the individual tack force pull-offs provided by the ISIT, Fig. 21 and equation [12],

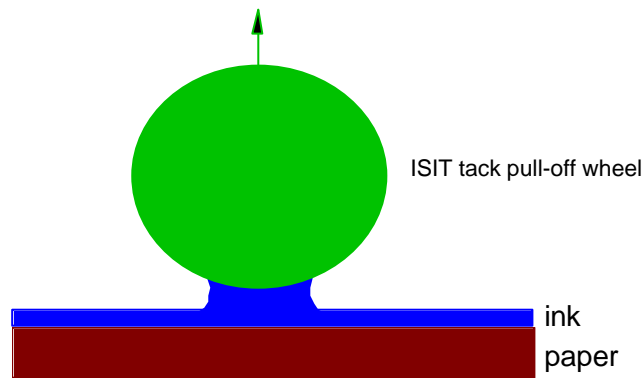


**Fig. 21** Tack pull-off geometry.

$$\mathbf{h}_p = \frac{\int F(t) dt}{A_F} \quad [12]$$

where  $A_F$  is the footprint area formed by the contact of the tack wheel with the paper surface. The obtained expression has the units of viscosity (a "process" viscosity,  $\mathbf{h}_p$ ) and is plotted in Fig. 22, where each pull-off curve has the form similar to that shown in Fig. 23.

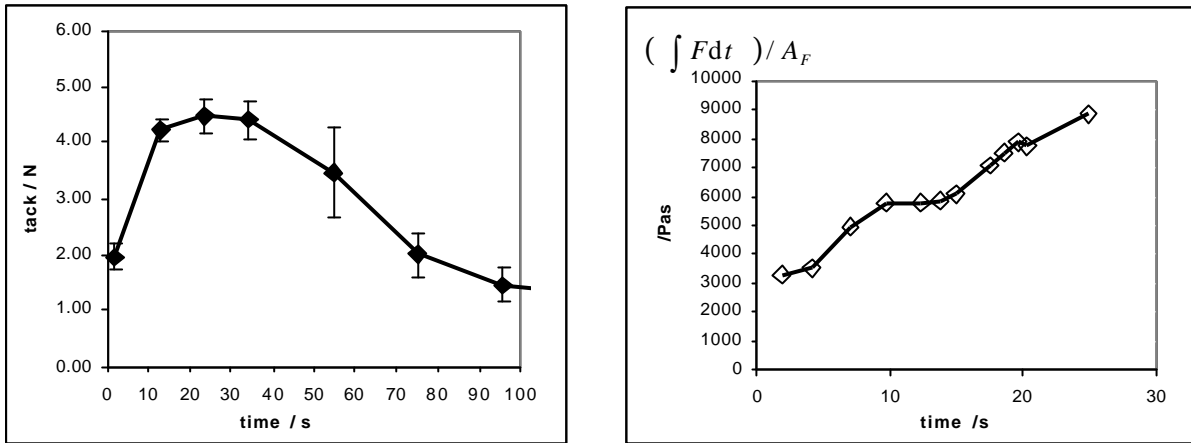


**Fig. 22** Overall mean tack curve for test paper and the tack rise in the form of a “process viscosity”.

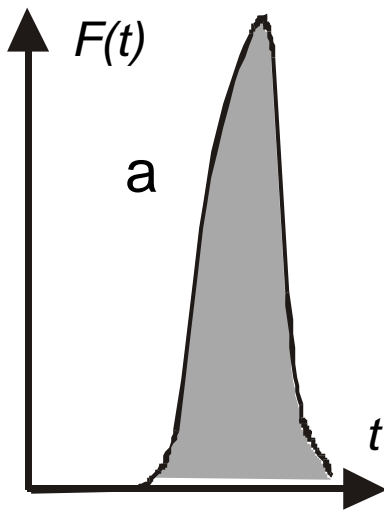


**Fig. 23** Schematic pull-off curve with integrated area.

Combining the Trouton ratio assumption (extensional viscosity = 3 x shear viscosity) with an independent rheological measurement of the ink viscosity as a function of oil dilution, a definition of the change in weight fraction of the oil content is obtained in relation to the footprint area  $A_F$ ,

$$\Delta f_{oil} \approx \frac{\ln \left( \frac{\int F(t) dt}{3A_F} k \right) - a}{b} \quad [13]$$

where  $k$  is a scaling factor between the process viscosity and the measured shear viscosity,  $a$  and  $b$  are the fitting parameters from the independent measurement of complex viscosity as a function of mineral oil content. The values are plotted in Fig. 24 for the tack data of Fig. 22 showing the time dependent decrease in oil content of the ink.

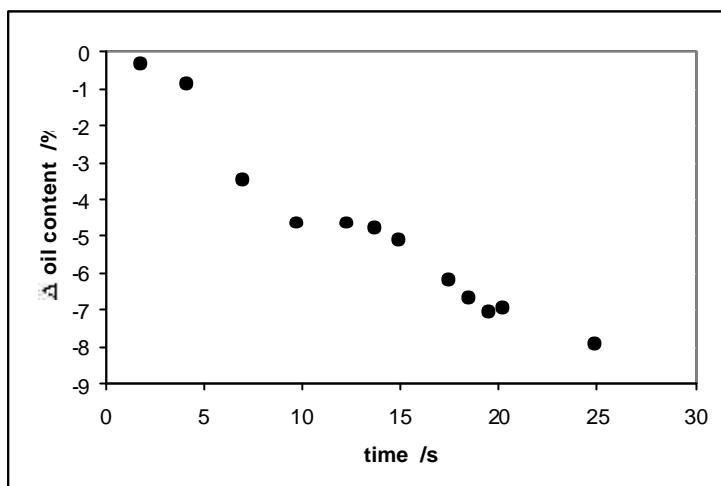


**Fig. 24** The proposed differential mineral oil weight fraction content of the ink from Eq. 12 as a function of time in contact with the paper surface.

The weight fraction of mineral oil content left in the ink is decreasing linearly with time over the timescale of tack increase (Fig. 24) as it becomes absorbed into the paper. This is an interesting finding, in that absorption of free fluid over such timescales would normally be expected to follow a  $\sqrt{t}$  relationship if Lucas Washburn applied. In fact, the rate of loss of oil mass from the printed ink layer is found to fall off as  $t^{-2}$ .

## FUTURE TRENDS

Pigment development is today a dynamic field. The economic driving forces in the paper industry more than ever before demand either one of two approaches or a combination of both: (i) continued development of the economy of scale we have seen over the past ten years, with mergers, consolidations and high speed, high volume, equipment, (ii) innovation. Many traditional sectors are open for innovation. Here we concentrate briefly on the future for pigmentation in InkJet and so-called digital papers.

### *Coated InkJet and Digital papers*

Copy papers form a commodity under increasing price competition. The high quality of uncoated copy grades today with ultrahigh brightness, bulk and stiffness can no longer be developed further along traditional lines. The door is open for an improved grade through the use of coating. A number of solutions are already becoming available, ranging from new forms of surface modified calcium carbonates and clays through to colloidal precipitated calcium carbonate, all targetted at full or part replacement of high cost precipitated silicas in inkjet applications. Commercial results from surface enhanced aluminosilicate and specially structure surface-modified calcium carbonates have been shown to reduce lateral ink spread and strikethrough. An example of a calcium carbonate pigment structure derived to develop internal pore volume and rapid absorbency is shown in Fig. 25. Such a pigment with a designed surface area of  $\sim 75 \text{ m}^2\text{g}^{-1}$ , provides high adsorbency for polymers and dyes, and effects a strong toner adhesion in laser printing.

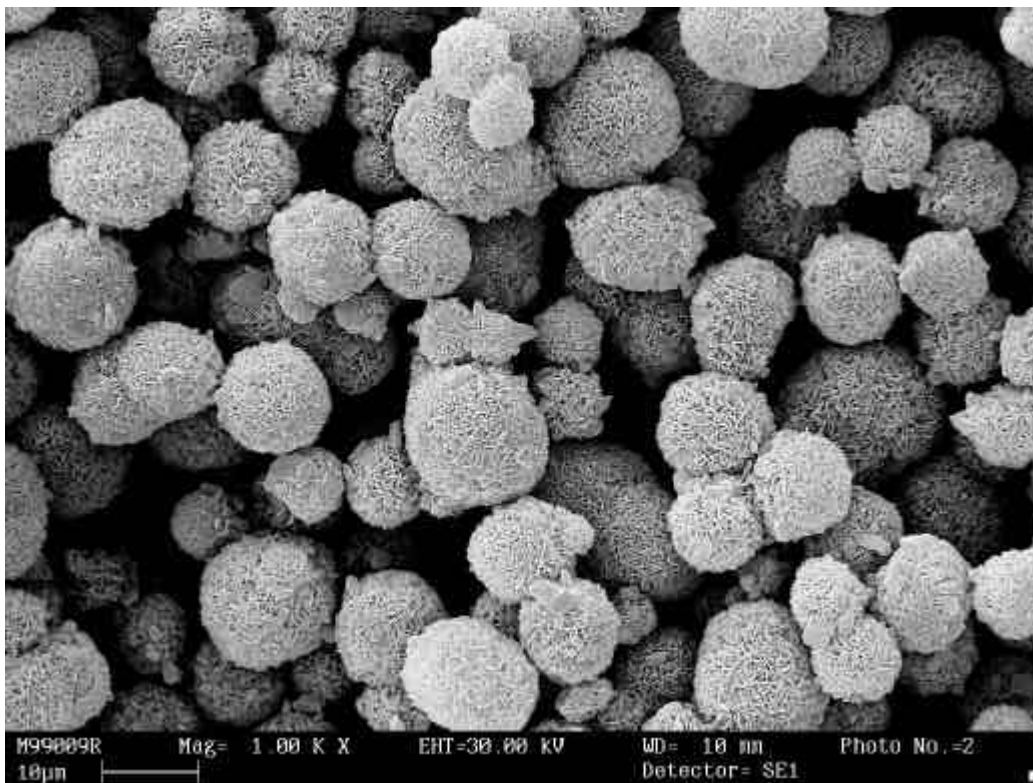


**Fig. 25** Electron micrograph of modified natural ground calcium carbonate designed for maximum absorption rate based on the absorption criteria discussed previously.

These concepts are also suitable for avoiding the use of internal sizing by using high surface area pigments as fillers and as coatings. The internal absorption capacity acts to capture ink and prevent strikethrough - a role traditionally played by the internal sizing to stop wicking along fibres.

Coating colour solids content for some of these newly developing grades is relatively low, and with speciality binders and polymers silicas today are coated at ~ 20-25 % w/w. Some of the newest proposals target ~ 50 % w/w. The metered sizepress is an ideally suited coater technology for such applications.

*High surface area pigments as fillers for metered sizepress coating basepapers*

The possibility of developing rapid absorption properties with respect to water and low viscosity oils by concentrating the pore size distribution of porous media within the 0.05 to 0.1 µm region gives new opportunities for designing the basepaper pore structure using pigments with internal pore volume. This leads to a concentration, as previously discussed, of the otherwise differentiating preferred pathway dynamic of absorption caused by inertial retardation during short timescale imbibition into larger pores. Not only, therefore, can we consider competitive absorption strategies in respect to printing but also in respect to promoting effective coating colour dewatering without impulse pressures by drawing the water phase into these filler structures as they might be used to fill basepapers. This concept is shown schematically in Fig. 26.

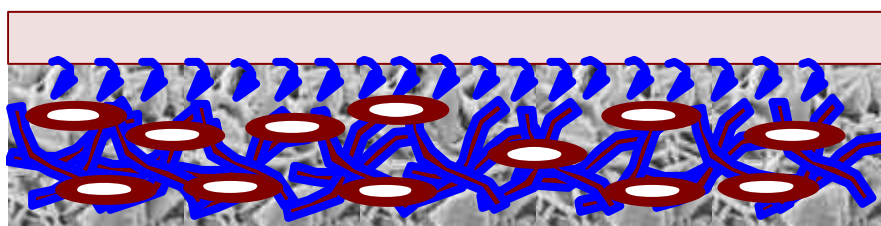


**Fig. 26** Absorption following the inertial pathway model promoting immobilisation of a coating layer.

### *A future in post-coating treatment?*

Surface chemistry plays a determining role in interactions with both existing and emerging printing technologies. To introduce novel surface chemistry modifications in conventional suspensions is extremely difficult and moves against the already accepted optimisation of dispersions and rheological properties of coating colours. Why not use the metered sizepress, say, to apply solutions of chemicals and/or polymer dispersions directly onto a preformed coating layer? This could, for example, encompass the cationisation of anionically dispersed coatings, obviating the need to develop specialised cationically dispersed pigments and binders. Barrier layer coatings could be made from polymer films applied to conventional coated grades. The opportunities seem endless, the innovation amongst our scientific and engineering community needs awakening to take advantage of the rapid tools for change that are available.

### *Economy the ever-present driver*

Papermakers today are using up to 30 % ground calcium carbonate filler in uncoated woodfree office papers. The statistics show that the average filler level in uncoated grades is 18 % in Europe and 12 % in the United States of America. The reason for the lower levels of filler is that a lot of grades suffer detrimental effects as filler loading increases; for example, loss of stiffness, bulk and strength. However, imagine the potential savings when using pigments that allow the highest possible filler loading in a specific grade rather than being limited by existing pigment strategies. Let us focus on the example of the U.S. paper industry: there are currently 11 million tons of uncoated fine paper produced in the U.S. at the average filler loading, quoted above, of 12 %. The following table shows the potential savings for this industry based on a pulp price of \$700 per ton and a filler price of \$150 per ton with a consequent replacement differential of \$700 - \$150 = \$550 per ton:

Raising filler loading	Potential savings in millions of \$
From 12 % to 18 %	363
From 12 % to 25 %	786
From 12 % to 30 %	1,089

Compromise on properties is even possible at these savings. New technologies for improving the structural properties of fillers such that they contribute to paper strength rather than detract must be an area for future development.

### **References used as background to this lecture and for recommended further reading**

1. Matthews, G.P., Ridgway, C.J. and Small, J.S., *Mar. Petrol. Geo.* **13**, 581 (1996).
2. Ridgway, C.J., Ridgway, K. and Matthews, G.P., *J. Pharmacol.* **49**, 377 (1997).
3. Peat, D.M.W., Matthews, G.P., Worsfield, P.J. and Jarvis, S.C., *Eur. J. Soil. Sci.* **51**, 56 (2000)
4. Ridgway, C.J., Schoelkopf, J., Gane, P.A.C. and Matthews G.P., "*The effects of void geometry and contact angle on the absorption of liquids into porous calcium carbonate pigmented structures*", paper submitted to Journal of Colloid and Interface Science (2000).
5. Schoelkopf, J., Ridgway, C. J., Gane, P. A. C., Matthews, G. P., and Spielmann, D. C, "*Measurement and network modelling of liquid permeation into compacted mineral blocks*", Journal of Colloid and Interface Science, **227**, 119-131 (2000).
6. Rousu, S.M., Gane, P. A. C., Spielmann, D. C, and Eklund, D, "*Separation of off-set ink components during absorption into pigment coating structures*", Paper and Coating Chemistry Symposium, Stockholm 2000, Nordic Pulp and Paper Research Journal, to be published.
7. Rousu, S.M., Gane, P.A.C., Spielmann, D.C. and Eklund, D.E., "*Differential absorption of offset ink components on coated paper*", Paper presented at the International Printing and Graphic Arts Conference, Savannah, GA, Proceedings, Tappi Press, tappi, Atlanta, GA.
8. Gane, P.A.C., Schoelkopf, J. and Matthews, G.P., "*Coating imbibition rate studies of offset inks: a novel determination of ink-on-paper viscosity and solids concentration using the ink tack force-time integral*", Paper presented at the International Printing and Graphic Arts Conference, Savannah, GA, Proceedings, Tappi Press, tappi, Atlanta, GA.
9. Schoelkopf, J., Gane, P. A. C., Ridgway, C. J., and Matthews, G. P., "*Influence of inertia on liquid absorption into paper coating structures*", Paper and Coating Chemistry Symposium, Stockholm 2000, Nordic Pulp and Paper Research Journal, to be published.

10. Gane, P.A.C., "*Coating structure: advancing the coating design for the print media of today and the challenges of the future*", Paper and Coating Chemistry Symposium, Stockholm 2000, Nordic Pulp and Paper Research Journal, to be published.
11. Gane, P. A. C., Schoelkopf, J., Spielmann, D. C., Matthews, G. P., and Ridgway, C. J., "*Observing fluid transport into porous coating structures: some novel findings*", Tappi Journal, 85(5), 2000, p1-3 (complete paper can be downloaded from the Tappi website).
12. Lucas, R. (1918): Kolloid Z. 23:15.
13. Washburn, E. W., "*The dynamics of capillary flow*", Physical Review, 17(1921), p273-28.
14. Bell, J.M., Cameron, F.K., "*The flow of liquids through capillary spaces*", Journal of Physical Chemistry, 10, 658. (1906).
15. Ostwald, W. (1908): Koll. Zeitschrift, *Suppl. Heft II*.
16. Quéré, D., "*Inertial capillarity*", Europhysics Letters, 39(5), 1997, p533-538
17. Kent, H.J., Lyne, M.B. (1989): "Influence of Paper Morphology on Short Term Wetting and Sorption Phenomena", Proceedings of the 9<sup>th</sup> Fundamental Research Symposium, Cambridge, U.K., Mech. Eng. Pub., Vol. 2, p895-920.
18. Gane, P.A.C., Buri, M. and Blum, R. "*Pigment co-structuring: new opportunities for higher brightness coverage and print-surface design*", International Symposium on Paper Coating Coverage, AEL METSKO, Helsinki, February 1999.
19. Gane, P.A.C. and Ridgway, C.J. "*Absorption rate studies of flexographic ink into porous structures: relation to dynamic polymer entrapment during preferred pathway imbibition.*", Paper presented at the 27<sup>th</sup> IARIGAI Research Conference, Graz, Austria 10-13 September 2000.
20. Moir, W.W., (1994), "*Flexography - A Review*", JOCCA-Surface Coatings International, 77, 221.
21. Xiang, Y. and Bousfield, D. W., "*The influence of coating structure on ink tack development*", Pan-Pacific and Printing & Graphic Arts Conference, CPPA, Canada, 1998, p93-101.
22. Desjumeaux, D., Bousfield, D. W., Glatter, T. P., Donigian, D. W., Ishley, J. N., Wise, K. J., (1998), "*Influence of Pigment Size on Wet Ink Gloss Development*", Journal of Pulp and Paper Science, 24, 150.
23. Gane, P.A.C., Kettle, J.P., Matthews, G.P. and Ridgway, C. J., "*Void space structure of compressible polymer spheres and consolidated calcium carbonate paper-coating formulations*", Industrial Engineering and Chemical Research 35, 1753 (1996).
24. Frith, W. J., Strivens, T. A., Mewis, J., "*Dynamic Mechanical-Properties of Polymerically Stabilized Dispersions*", Journal of Colloid and Interface Science, 139, 55(1990).
25. Gane, P. A. C., Seyler, E. N., and Swan, A., "*Some Novel Aspects of Ink/Paper Interactions in Offset Printing*", Printing and Graphic Arts Conference, Halifax, Nova Scotia CPPA, Montreal, Canada, 1994, p209-228.
26. Bosanquet, C. M., "*On the flow of liquids into capillary tubes*", Phil.Mag., S6 45(267), 1923, p525-531.